Resources, Conservation & Recycling 223 (2025) 108520

Contents lists available at ScienceDirect

Resources, Conservation & Recycling

journal homepage: www.sciencedirect.com/journal/resources-conservation-and-recycling

Avoided CO_2 emissions in China's power sector by structural change and efficiency gain: An electric generating unit level analysis

Chao Zhang [a,b,c,*], Yujie Dong [a], Lijin Zhong [d,*], Haoqi Qian [e,*], Shuangtong Wang [f], Gang He [g,h,i]

[a] School of Economics and Management, Tongji University, Shanghai, 200092, China
[b] United Nation Environment-Tongji Institute of Environment for Sustainable Development, Tongji University, Shanghai, 200092, China
[c] Research Institute for Carbon Neutrality, Tongji University, Shanghai, 200092, China
[d] Huanding Environmental Big Data Institute, Beijing, 100083, China
[e] Institute for Global Public Policy, Fudan University, Shanghai, 200433, China
[f] Energy Science and Technology Research Institute Co., Ltd, Nanjing, 210023, China
[g] Marxe School of Public and International Affairs, Baruch College, City University of New York, New York, 10010, USA
[h] CUNY Institute for Demographic Research, City University of New York, New York, 10010, USA
[i] Earth and Environmental Sciences, The Graduate Center, City University of New York, New York, 10016, USA

ARTICLE INFO

Keywords:
Power sector
CO_2 emission
Bottom-up accounting
Decomposition analysis
China

ABSTRACT

In this study, we compile a comprehensive time-series bottom-up dataset of heat rate and CO_2 emission at the electric generating unit (EGU) level for China's power sector, and decompose contributions of various technological factors to CO_2 emission reduction. Results show that dramatic structural change and efficiency gain have reduced the national average CO_2 intensity of final electricity consumption from 983.3 g CO_2/kWh in 1997 to 544.9 g CO_2/kWh in 2022, cumulatively avoiding 15.8 billion tonnes of potential CO_2 emission. Fuel mix adjustment (38.3 %, 6055 Mt), heat rate decrease (35.0 %, 5527 Mt), and upsizing of EGUs (23.2 %, 3661 Mt) are the top three factors for CO_2 mitigation. Decomposition analysis based on the bottom-up dataset captures detailed technological and structural changesat the EGU level, enabling a more precise evaluation of the effects of alternative decarbonization policies. As potentialfor energy efficiency improvement of traditional coal-fired power generation is shrinking, future policies should focus on new areas of low-carbon retrofits.

1. Introduction

China is the world's largest emitter of carbon dioxide (CO_2), accounting for 28 % (11.5 gigatonnes, Gt) of the global total in 2022 (IEA, 2023). Fossil fuel-fired power generation (mainly coal power) roughly contributes two-thirds of China's total electricity production and is responsible for 41 % of the national total CO_2 emissions (4.72 Gt in 11.5 Gt as of 2022) (CEC China Electricity Council, 2023; Jia et al., 2023). Decarbonizing the power sector is crucial to achieving China's climate ambitions of peaking carbon emissions before 2030 and attaining carbon neutrality before 2060 (Liu et al., 2022).

While Western European countries and the United States have accelerated the decommissioning of aged and carbon-intensive fossil fuel-fired power plants (GEM, 2022; Heinrichs and Markewitz, 2017; EIA, 2019), China faces a unique challenge of much younger coal power plants on duty. with a total of 331 GW coal power units built in China after the announcement of the Paris Agreement (during 2015–2022) (GEM, 2022). The relatively young age structure of coal power plants presents obstacles to achieving an earlier and lower peak in emissions (von Dulong, 2023; Wang et al., 2020a). On the other hand, the dynamically growing power generation fleet also provides great opportunities for technological advancements in both emerging renewable power technologies and traditional fossil fuel-fired electric generating units (EGUs).

Notably, the fuel consumption factor of thermal power generation in China has significantly decreased over the past two decades. According to statistics from the China Electricity Council (CEC), the national average heat rate of thermal power generation has decreased from 394 g of coal equivalent per kilowatt-hour (gce/kWh) in 2000 to 300.7 gce/kWh in 2022, by 23.7 %. This improvement has correspondingly reduced CO_2 intensity by 259.4 g CO_2/kWh (CEC China Electricity

* Corresponding authors.
E-mail addresses: chao_zhang@tongji.edu.cn (C. Zhang), zhonglijin@huanding.org (L. Zhong), qianhaoqi@fudan.edu.cn (H. Qian).

https://doi.org/10.1016/j.resconrec.2025.108520
Received 7 October 2024; Received in revised form 5 June 2025; Accepted 16 July 2025

Nomenclature

Acronyms

EGU	Electric generating unit
CEC	China electricity council
CHP	Combined heat and power
HER	Heat to electricity supply ratio
LCV	Lower calorific value

Variable

$HR_{i,t}$	The heat rate of EGU i in year t
T, t	Year variable and index
$UT_{u,i}$	Dummy variable indicating whether EGU i belongs to unit type u
$CT_{c,i}$	Dummy variable indicating whether EGU i uses cooling technology c
$X_{HER,i,t}$	The heat to electricity supply ratio of EGU i in year t
$X_{CF,i,t}$	The capacity factor of EGU i in year t
$X_{TEMP,i,t}$	The yearly average temperature of the location of EGU i in year t
$X_{LCV,i,t}$	The lower calorific value of EGU i in year t
$PROV_i$	Dummy variable indicating the province where EGU i is located
$CE_{i,t}$	The total CO_2 emission by EGU/power plant i in year t
$NEG_{i,t}$	The net electricity generation by EGU/power plant i in year t
$CI_{i,t}$	The CO_2 intensity of net electricity generation by EGU/power plant i in year t
EF_i	The CO_2 emission factor of the fuel used by EGU/power plant i
CCF_i	The carbon content factor of the fuel used by EGU/power plant i
COF_i	The carbon oxidation factor of the fuel used by EGU/power plant i
TED	Total electricity demand
LL	Grid line loss rate of electricity supply
FM_j	The percentage of net electricity generation using fuel j
UT_{jk}	The percentage of unit type k in net electricity generation by fuel j
CT_{jkl}	The percentage of cooling technology l in net electricity generation by fuel j *and* unit type k
CHP_{jklm}	The percentage of CHP (or non-CHP) unit type m in net electricity generation by fuel j, unit type k and cooling technology l

Parameters

α	Constant term
β_u	The regression coefficient for unit type
$\beta^{'}_u$	The regression coefficient for the interaction term of unit type and year of operation
$\beta^{''}_u$	The regression coefficient for the interaction term of unit type and the quadratic term of year of operation
$\gamma_{c,u}$	The regression coefficient of the interaction term of cooling technology and unit type
$\gamma^{'}_{c,u}$	The regression coefficient of the interaction term of cooling technology, unit type and year of operation
θ_n	The regression coefficients of the control variables
$\theta^{'}_n$	The regression coefficients of the interaction terms of control variables and year of operation
μ_i	The regression coefficient of province fixed effect
$\varepsilon_{i,t}$	Error term

Council, 2023; SETC, 2001). These substantial enhancements in energy efficiency have played a critical role in mitigating the growth of coal consumption and CO_2 emissions, when electricity demand continues to surge.

Many previous studies have investigated the driving factors of CO_2 emission reduction in China's power sector based on decomposition analysis. As shown in the following Literature Review section, almost all of these studies adopted top-down frameworks, which rely on macro-level statistic data. Reduction in the average heat rate of thermal power generation was usually treated as an aggregated factor in the decomposition analysis. However, the achievements in energy efficiency improvement can be attributed to various policy interventions aiming at regulating and guiding different aspects of technology innovation and investment in the power industry (Li et al., 2019; Zhang et al., 2016, 2020; Zhang et al., 2022), for example, phasing out outdated generation capacities, raising coal consumption standards for new power plants, financing energy efficiency retrofits, and improving power transmission and distribution efficiency. Understanding the contributions of different technological factors to energy conservation and emission reduction helps to evaluate the effectiveness of alternative policies and inform future decarbonization pathways. Since aggregate statistics cannot reveal structural and efficiency changes of power generation in detail, collecting and compiling high-quality bottom-up information is crucial for filling the knowledge gap. Given the large scale of China's power sector and diverse technological characteristics in different regions, this work is extremely laborious and challenging.

In this study, we developed a comprehensive time-series bottom-up inventory that encompasses power generation, heat rate and CO_2 emission at the electric generating unit (EGU) level of China's power sector, covering the period from 1997 to 2022. To the best of our knowledge, this dataset is the most comprehensive one of its kind so far. It enables us to attribute changes in CO_2 emissions to detailed technological factors in a bottom-up manner. Heterogeneity in heat rate and emission intensity of different EGU types in different regions can be fully incorporated into decomposition analysis. Our findings provide new information regarding significant structural changes and efficiency gains especially within China's coal power sector over the past 26 years. These results cannot be obtained from previous studies based on aggregate top-down statistic data, which only show changes in the average heat rate or emission intensity of the entire coal power sector. We reveal that while CO_2 emissions from power generation was increasing continuously, a relative decoupling between electricity production and the associated CO_2 emissions has been achieved. A five-fold rise in the total CO_2 emissions has supported a more than eight-fold increase in the total electricity demand. The effects of the reduction in line losses, changes in the fuel mix, shifts in EGU mix, and decrease in heat rate for all unit types have collectively offset 23.4 % (15.8 billion tonnes CO_2) of the potential growth in cumulative emissions since 1997. The dominant driving factors vary by province, exhibiting a spatial cluster feature.

The rest of the paper is organized as follows: Section 2 reviews relevant studies on decomposition analysis of CO_2 emissions in power sector, Section 3 introduces the processes of compiling the time-series bottom-up EGUs dataset, Section 4 presents the results of decomposition analysis at both national and provincial level, Section 5 discusses policy implications of our analysis, and Section 6 summarizes main conclusions.

2. Literature review

Over the past decade, significant attention has been given to decomposing CO_2 emissions in the power sector, particularly in exploring the factors driving emission trends and guiding policy decisions. We compare 30 peer-reviewed studies published since 2010 investigating these driving factors. Table 1 provides an overview of the core features of these studies, including their scope, time span, method, data resolution and identified driving factors of emissions in the power sector.

2.1. Research scope

The research scope of this topic spans country, continent, and global levels. Most studies concentrate on individual countries, with a significant focus on China. Country-level analyses also cover developed nations such as the United States (Mohlin et al., 2019) and Canada (Steenhof and Weber, 2011), as well as developing countries like Pakistan (Raza and Lin, 2022) and Bangladesh (Hasan and Chongbo, 2020). Continental studies investigate regions such as the European Union (Karmellos et al., 2021; Rodrigues et al., 2020; Karmellos, et al., 2016) and Asia (Ang and Goh, 2016; Goh and Ang, 2020). At a broader scale, global-level studies (Qin et al., 2022; Goh et al., 2018; Ang and Su, 2016) examine trends across multiple countries or regions.

2.2. Research methods

We concentrate on articles that employ the index decomposition analysis (IDA) method. Among these, the Logarithmic Mean Divisia Index (LMDI) method stands out as the most commonly used approach because of its sound theoretical basis and ability of complete decomposition (Goh et al., 2018). Additionally, a few studies employ the Generalized Divisia Index Method (GDIM) (Yan et al., 2019a; 2019b), Theil index (Wang et al., 2020) and Lespeyres method (Steenhof and Weber, 2011). LMDI method has many merits compared to other methods. It can fully decompose changes in the aggregated indicator without unexplained residual. Results can be additively aggregated, so that sub-sector decompositions can be summed up to the total, keeping consistent across different levels (Ang et al., 2003). It also handles zero values properly due to its logarithmic weighting scheme (Ang and Liu, 2001).

2.3. Data resolution

As summarized in Table 1, almost all existing studies rely on top-down macro-level statistic data for decomposition analysis at national, regional or provincial level. These studies often span long time periods, enabling them to capture broad trends in power sector CO_2 emissions and their responses to policy changes from a macro perspective. Bottom-up unit-level data has only been used by Qin and colleagues (Qin et al., 2022) as part of the global-level analysis of CO_2 emissions in the power sector. However, their focus remained on activity level, fuel mix, and heat rate, with less attention given to structural changes in electric generating units. The substantial contribution of unit-level structural changes in the power sector, such as the replacement of small units with larger ones, shifts in fuel types, and changes in cooling technologies, to national CO_2 emission reductions has not been adequately revealed.

2.4. Driving factors

The extent to which driving factors can be thoroughly identified and differentiated is largely determined by the granularity of the available data. And the results of decomposition analyses can vary significantly based on the selection of driving factors (Goh et al., 2018). These driving factors can be broadly categorized into demand-side and supply-side factors.

From the demand side, macroeconomic factors such as GDP, electricity consumption, and energy intensity are commonly selected, often using analytical frameworks such as the IPAT equation (Ehrlich and Holdren, 1971) or Kaya identity (Kaya, 1995). These studies typically interpreted overall changes in CO_2 emission to factors as the outcome of population growth, increases in per capita GDP (level of affluence), changes in electricity demand per unit GDP (energy intensity) and average heat rate or CO_2 intensity per kWh electricity generation (technology efficiency). As summarized in Table 1, approximately half of the reviewed studies (14 out of 30) consider demand-side indicators in their decomposition analyses. The findings of these studies consistently showing that while population growth and economic expansion contribute to increased CO_2 emissions, reductions in energy intensity and improvements in technological efficiency have a mitigating effect (Zheng et al., 2020; Xie et al., 2019; Chen et al., 2018).

Technological efficiency in the power sector is commonly represented by CO_2 emission intensity on the production side. As summarized in Table 1, all of the reviewed studies adopt this indicator in their analyses. In addition, changes in the fuel mix are also frequently incorporated as a key decomposition factor in the majority of analyses. Specifically, 22 studies distinguished between different fuel types for thermal power generation, while 5 studies focused exclusively on the share of thermal power. These studies calculate average emission intensities for coal power or thermal power as a whole, reflecting changes in fuel mix and thermal efficiency. However, variations in the fuel mix within the thermal power sector, such as shifts in fuel composition between coal, natural gas, and oil, have received limited attention in the existing literature. Moreover, none of these existing studies have investigated the CO_2 mitigation effect of significant dynamic changes in the structure of EGUs and their technological progress.

2.5. Summary

In summary, while extensive research exists in this area, most studies rely on macro-level analysis using top-down data and aggregated indicators. Such approaches are constrained by their broad scope and limited granularity, which can obscure nuanced technological progress and operational enhancements. Specifically, various factors that exert notable influence on the energy efficiency of units tended to become conflated, such as the deployment of large-sized units, switching cooling technologies, and improvement in thermal efficiency of specific unit types (EIA, 2015). A more detailed analysis is therefore essential to differentiate and quantify the effects of policies triggering different technological changes in China's power sector. Moreover, substantial regional disparities exist in emission trajectories and their driving factors due to variations in the technology mix of generation capacity, shaped by local energy resource endowments and region-specific regulatory constraints. To address these gaps, this study compiled a time-series EGU-level bottom-up dataset for decomposing CO_2 emissions in China's power sector, capturing structural and efficiency changes in generating units and enabling a more detailed assessment of policy impacts on power sector decarbonization.

3. Data and methods

3.1. EGU database

The EGU/power plant database used in this study is extensively extended from a previous work on water use inventory of China's thermal power sector by Zhang and colleagues (Zhang et al., 2018). The database in this study covers all generation technologies, a longer time span from 1997 to 2022, and more detailed information on fuel consumption at the power plant and EGU levels. Technological and operational indicators for each EGU/power plant include geographic location, year of commissioning and decommissioning (if applicable), fuel type, nameplate capacity, prime mover, boiler pressure level, cooling technology, heat-to-electricity ratio of combined heat and power (CHP) plants, yearly utilization hours, gross and net power generation, auxiliary power consumption rate, lower calorific value of coal, heat rate, and yearly average ambient temperature. In this study, heat rate (i.e., fuel

Table 1
Comparison between this study and previous ones.

Study	Time span	Scope	Method	Data resolution	Driving factors									
					Demand side	Production side								
						ACT	CI							
							CI without decomposition	Decomposition of CI						
								LL	FM		UT	CT	CHP	HR
									Fuel types	Thermal only				
This study	1997 - 2018	China	LMDI	Bottom-up unit level data	–	√	–	√	√	–	√	√	√	√
He et al., 2022	2005 - 2019	China	LMDI	Top-down provincial level data	√	–	–	–	√	–	–	–	–	√
Raza et al., 2022	1990 - 2019	Pakistan	LMDI	Top-down national level data	√	–	√	–	–	–	–	–	–	–
Wang et al., 2022	2000 - 2019	China	LMDI	Top-down provincial level data	√	–	–	–	√	√	–	–	–	√
Qin et al. , 2022	1990 - 2019	Global	LMDI	Bottom-up unit level data	–	√	–	–	√	–	–	–	–	√
Karmellos et al., 2021	2000 - 2018	European Union	LMDI	Top-down national level data	–	–	–	–	√	–	–	–	–	√
Wang et al., 2021	1997 - 2017	China	LMDI	Top-down provincial level data	–	√	–	–	√	√	–	–	–	√
Zhao et al., 2020	2001 - 2015	China	LMDI	Top-down provincial level data	–	–	–	–	√	√	–	–	–	√
Hasan et al., 2020	1979 - 2018	Bangladesh	LMDI	Top-down national level data	√	–	–	–	–	√	–	–	–	√
Goh et al., 2020	2000 - 2015	ASEAN	ST-IDA	Top-down national level data	–	–	–	–	–	√	–	–	–	√
Wang et al., 2020	2000 - 2016	China	Theil index	Top-down provincial level data	–	–	–	–	√	–	–	–	–	√
Rodrigues et al., 2020	2000 - 2015	European Union	LMDI	Top-down national level data	√	–	–	–	√	√	–	–	–	√
Zheng et al., 2020	1978 - 2018	China	LMDI (Kaya identity)	Top-down national level data	√	–	√	–	–	–	–	–	–	–
Liao et al., 2019	2005 - 2015	China	LMDI	Top-down provincial level data	√	–	–	√	–	√	–	–	–	√
Xie et al., 2019	1985 - 2016	China	LMDI (Kaya identity)	Top-down national level data	√	–	–	√	√	√	–	–	–	√
Yan et al., 2019a	2000 - 2016	China	GDIM	Top-down regional power grid level data	√	√	√	–	–	–	–	–	–	–
Yan et al., 2019b	2000 - 2016	China	GDIM	Top-down provincial level data	–	√	–	–	√	–	–	–	–	√
Mohlin et al., 2019	1990 - 2005	USA	LMDI	Top-down state level data	–	√	–	–	√	–	–	–	–	√
Chen et al., 2018	2003 - 2015	China	LMDI (Kaya identity)	Top-down national level data	√	–	–	–	√	–	–	–	–	√
Wang et al., 2018	1995 - 2014	China	LMDI	Top-down provincial level data	–	–	–	–	√	√	–	–	–	√
Peng et al., 2018	1980 - 2014	China	LMDI	Top-down national level data	–	–	–	–	–	√	–	–	–	√
Goh et al., 2018	1990 - 2014	Global	LMDI	Top-down global and	–	–	–	–	√	√	–	–	–	√

(continued on next page)

Table 1 (*continued*)

Study	Time span	Scope	Method	Data resolution	Driving factors									
					Demand side	Production side								
						ACT	CI							
							CI without decomposition	Decomposition of CI						
								LL	FM		UT	CT	CHP	HR
									Fuel types	Thermal only				
				national level data										
Liu et al., 2017	2000 - 2014	China	LMDI	Top-down provincial level data	–	–	–	–	√	√	–	–	–	√
Yang et al., 2016	1985 - 2011	China	LMDI	Top-down national level data	√	–	–	–	–	√	–	–	–	√
Yan et al., 2016	2000 - 2012	China	LMDI	Top-down power grid level data	√	–	–	–	√	–	–	–	–	√
Karmellos et al., 2016	2000 - 2012	European Union	LMDI	Top-down national level data	√	–	–	–	√	–	–	–	–	√
Ang et al., 2016a	1990 - 2013	ASEAN	LMDI	Top-down national level data	–	–	–	–	√	√	–	–	–	√
Ang et al., 2016b	1990 - 2013	Global	LMDI	Top-down national level data	–	–	–	–	√	√	–	–	–	√
Zhou et al., 2014	2004 - 2010	China	LMDI	Top-down power grid level data	–	√	–	–	√	–	–	–	–	√
Zhang et al., 2013	1991 - 2009	China	LMDI	Top-down national level data	√	–	–	–	√	√	–	–	–	√
Steenhof et al., 2011	1990 - 2008	Canada	Lespeyres	Top-down provincial level data	–	√	–	√	√	–	–	–	–	√

Notes: On the **demand side** includes electricity consumption, economic scales and population and so on; On the **production side, *ACT*** refers to electricity output, ***CI*** refers to the CO_2 intensity of the power sector. ***LL*** refers to grid line loss rate in power transmission and distribution, ***FM*** refers to fuel mix structure, ***UT*** refers to unit type changes in thermal power generation, ***CT*** refers to cooling technology structure and ***CHP*** refers to the share of combined heat and power units. In the ***FM*** part, "fuel types" refers to studies that differentiate various combustible fuels, and "thermal only" refers to studies that use only the share of thermal power generation as an indicator of fuel mix.

consumption per kWh net power generation) for each plant and EGU is the most important indicator supplemented into the database. Various data sources are compiled and cross-checked, including: 1) a complete list of coal-fired EGUs equipped with desulfurization facilities published by the Chinese Ministry of Environmental Protection (MEP, 2014); 2) a complete list of all EGUs larger than 6 MW in operation in 2000 complied by the Chinese Electricity Council (CEC, 2001); 3) complete lists of newly commissioned EGUs larger than 6 MW for each year (CEC, 1997–2022); 4) complete lists of plant-level operational information for all power plants larger than 6 MW for each year (CEC, 1997–2022); 5) operational indicators at EGU-level from the Energy Efficiency Benchmarking Competition of coal-fired electric-generating units for 2008–2021 (CEC, 2008–2021).

Matching and harmonizing the plant-level and EGU-level technological and operational information for fossil fuel-fired power generation is the main task of database construction. All coal-fired EGUs with a nameplate capacity equal to or larger than 100 MW listed in data source 1, 2, 3 and 5 are matched with corresponding power plants listed in data source 4. Power generation, heat rate and CO_2 emission of these medium- and large-sized EGUs are identified and calculated separately. Small-sized EGUs (<100 MW) are also matched with corresponding power plants, but are classified as the same unit type. Plant-level power generation and heat rate are directly used in the calculation for small units. Thus, unit types are distinguished into nine categories according to nameplate capacity and boiler pressure, i.e., smaller than 100 MW, 100 MW class, 200 MW class, 300 MW class subcritical, 300 MW class supercritical, 600 MW class subcritical, 600 MW class supercritical, 600 MW class ultra-supercritical, and 1000 MW class ultra-supercritical. Natural gas-fired EGUs are categorized into three types according to the nameplate capacity and combustor temperature of the gas turbine, i. e., smaller than E class (< 100 MW), E class (100–200 MW) and F class (> 200 MW). Thermal power plants using other combustible fuels (e.g., oil, recovered gases, biomass, municipal solid waste and residual heat & pressure) usually have small installed capacity and are not disaggregated into EGUs and different unit types. Nuclear and renewable power generation, including hydropower, wind and solar PV, do not have CO_2 emissions. National and provincial aggregate power generation by nuclear and renewable power plants are used in the calculation.

The annual Energy Efficiency Benchmarking Competition Report (data source 5) provides detailed technological and operational information of more than 1300 medium- and large-sized EGUs, accounting for approximately 60 % of the total capacity of coal-fired power generation. Missing technological information of EGUs that are not included in data source 5 are supplemented by searching the internet for open-source information. Cooling technology type can be visually identified from satellite images obtained from Google Earth software. Water-cooling and air-cooling units —can be distinguished based on the characteristics of cooling facilities. Specifically, recirculating cooling EGUs have cooling towers, and air-cooling EGUs are equipped with air-cooling islands. Once-through cooling EGUs do not have such structures, and are usually located beside rivers or lakes. Whether a power plant is a CHP plant is mainly identified by the presence of relevant keywords, such as “heat and power”, in its plant name or relevant description in official approval documents. For the installed capacity and classification of natural gas-fired units, information can usually be extracted from news reports about the commissioning of natural gas-fired power plants.

The compiled inventory includes nearly all EGUs or power plants with an installed capacity larger than 6 MW in China, allowing us to encompass almost all grid-connected power generation. In total, our database includes ~10,300 thermal power generating units/plants with a total installed capacity of ~1452 GW, comprised of over 9000 coal-fired EGUs (~1317 GW), 375 natural gas-fired EGUs (~105 GW) and more than 1000 power plants using other combustible fuels (~88 GW, including oil, recovered gases, biomass, municipal solid wastes and residual heat & pressure).

3.2. Operating heat rate and power generation at EGU/plant level

Heat rate represents the amount of energy input to generate one kilowatt hour (kWh) of electricity, measured in gram of coal equivalent per kWh electricity generation (gce/kWh). In order to make best use of available data sources, we use data with higher quality in priority. For coal-fired EGUs larger than or equal to 100 MW, there are three situations in data selection. First, if an EGU is included in the Energy Efficiency Benchmarking Competition, the reported heat rate and power generation are directly used in the calculation. Approximately 9900 samples of coal-fired EGUs with a nameplate capacity larger than 100 MW have been reported in the benchmarking competition since 2008 (Supplementary Table 1). Second, for an EGU that is not included in the benchmarking competition, if the power plant it belongs to has homogeneous unit type, we assign the plant-level heat rate reported in data source 4 to this EGU and equally disaggregate plant-level power generation to EGU-level. Third, if a coal-fired power plant has multiple medium- and large-sized EGUs (≥100 MW) with different unit types and/or cooling technologies, the plant-level heat rate cannot reflect the EGU-level heat rate. We then use a multiple regression model based on sample data from the benchmarking competition and power plants with single-type EGUs to estimate heat rate for different types of EGUs, as shown in Eq. (1). The multiple regression model takes into account key technological and operational factors that affect the energy efficiency of power generation, including unit type, cooling technology, heat-to-electricity ratio, capacity factor, lower calorific value of coal and ambient temperature. Time trend and provincial fixed effects are also considered in the model. We assume that power generation by an individual EGU is proportional to the share of its nameplate capacity in the total capacity of that plant.

$$
\begin{aligned}
\ln HR_{i,t} = \alpha + \sum_u \left(\beta_u + \beta'_u T + \beta''_u T^2\right) UT_{u,i} \\
+ \sum_{c,u} \left(\gamma_{c,u} + \gamma'_{c,u} T\right) CT_{c,i} UT_{u,i} \\
+ \sum_n \left(\theta_n + \theta'_n T\right) X_{n,i,t} + \mu_i PROV_i + \varepsilon_{i,t}
\end{aligned}
\tag{1}
$$

where $HR_{i,t}$ is the heat rate (measured in gce/kWh) of EGU i in year t, $UT_{u,i}$ is a dummy variable indicating whether EGU i belongs to unit type u, $CT_{c,i}$ is a dummy variable indicating whether EGU i uses cooling technology c, T is the year variable, $PROV_i$ is a dummy variable indicating the province where EGU i is located. All control variables are represented by $X_{n,i,t}$, including heat-to-electricity ratio $X_{HER,i,t}$, which is the ratio of heat supply to electricity supply of a combined heat and power generation unit (CHP), yearly capacity factor $X_{CF,i,t}$, which is calculated by dividing the yearly utilization hours by 8760 hours, ambient temperature $X_{TEMP,i,t}$, which is the yearly average temperature of the location of EGU i, and lower calorific value of coal $X_{LCV,i,t}$, which reflects the quality of the coal used for power generation by EGU i in year t. We define the base year 1997 as 1 for the year variable in the regression. α, β_u, β'_u, β''_u, $\gamma_{c,u}$, $\gamma'_{c,u}$, θ_n, θ'_n and μ_i are regression coefficients to be estimated.

The model is estimated by an ordinary least square method, with has a goodness-of-fit (R^2) of 0.775 (Supplementary Table 2). The regression result shows that larger unit size and higher boiler pressure lead to lower heat rate. Air cooling units have higher heat rate compared to the wet cooling counterparts. In addition, higher HER, higher capacity factor, higher LCV and lower ambient temperature are associated with lower heat rate.

For non-coal-fired thermal power generation (natural gas and all other combustible fuels), data of plant-level heat rate reported in data source 4 are directly used in our calculation. Our bottom-up database is quite comprehensive. On average, the yearly EGU-level electricity generation adds up to ~99 % of the top-down statistic data of China’s national total power generation (Supplementary Fig. 1).

3.3. Uncertainty assessment

Uncertainty analysis is necessary for ensuring the reliability and precision of bottom-up accounting. We assume that all reported heat rate values are certain and only the estimated values for a small part of coal-fired EGUs using the multiple regression model have errors. To quantify this uncertainty, we calculated the 95 % confidence intervals (CIs) for each predicted value. The confidence intervals derived from the regression analysis are then incorporated into the calculation of the group-averaged heat rate. The average heat rate of all types of coal-fired EGUs with 95 % CIs are presented in Supplementary Table 5. The confidence intervals are very small compared to the average heat rates (less than 0.1 % in most situations).

3.4. CO_2 intensity and CO_2 emissions

We derive EGU- and plant-level CO_2 intensity (measured in g CO_2/kWh) and CO_2 emissions (measured in tonnes) following guidelines from the Intergovernmental Panel on Climate Change (IPCC, 2006) and Guidelines for the Compilation of Provincial Greenhouse Gas Inventory issued by Chinese National Development and Reform Commission (NDRC, 2011):

$$
\begin{aligned}
\sum_i CE_{i,t} = NEG_{i,t} \times CI_{i,t} = NEG_{i,t} \times HR_{i,t} \times EF_i = NEG_{i,t} \times HR_{i,t} \times CCF_i \\
\times COF_i \times \frac{44}{12}
\end{aligned}
\tag{2}
$$

Where $CE_{i,t}$ refers to the total CO_2 emission by EGU/power plant i in year t, $NEG_{i,t}$ is net electricity generation by EGU/power plant i in year t, $CI_{i,t}$ is the CO_2 intensity (measured in g CO_2/kWh) of net power generation by EGU/power plant i in year t, $HR_{i,t}$ is the heat rate (measured in gce/kWh) of EGU/power plant i in year t, EF_i refers to CO_2 emission factor of the fuel used by EGU/power plant i (measured in g CO_2/gce), CCF_i refers to carbon content factor of the fuel used by EGU/power plant i (measured in g C/gce), COF_i refers to carbon oxidation factor of the fuel used by EGU/power plant i. The carbon content factor of coal (0.806 g C/gce), natural gas (0.449 g C/gce), oil (0.592 g C/gce) and recovered gases (0.398 g C/gce) as well as their carbon oxidation factors are derived from the Guidelines for the Compilation of Provincial Greenhouse Gas Inventory (NDRC, 2011). The carbon content factor of municipal solid wastes (0.733 g C/gce) is extracted from the IPCC guideline (IPCC, 2006). CO_2 emission from power generation by biomass combustion and residual heat and pressure is set as 0 (Supplementary Table 3).

3.5. Decomposition analysis

This study decomposed the changes in CO_2 emissions of China’s power sector into more detailed factors related to production-side technological structure and energy efficiency based on the bottom-up emission inventory. We first distinguish eleven types of fuel or renewable technologies in the analysis, including seven combustible fuels (coal, natural gas, oil, recovered gases, biomass, municipal solid wastes and residual heat & pressure) and four low carbon generation technologies (nuclear power, hydropower, wind turbine and solar PV). Then, coal-fired power generation is further classified into 36 categories according to three primary technological attributes that affect its energy efficiency, i.e., unit type (nine categories), cooling technology (wet or air-cooling), and CHP or non-CHP unit. Natural gas-fired EGUs are classified into three unit types based on the nameplate capacity of the units, i.e., smaller than 100MW, 100–200 MW (E-class), and larger than 200 MW (F-class). EGU-level or plant-level heat rate data compiled using the bottom-up approach are grouped by the above-mentioned technology categories for each year. Group-averaged heat rate can be calculated to reflect changes in generating efficiency over time in each technology category. Furthermore, we also take into account the impact of variations in the line loss rate during power transmission and dispatch, since lowering line loss helps to lower power generation to satisfy specific electricity demand.

We use the LMDI method (Ang et al., 2003) to decompose changes in CO_2 emissions into seven factors as shown in Eq. (3), i.e., changes in total electricity demand, line loss rate, fuel mix, unit type structure, cooling technology structure, share of CHP units and group-averaged heat rate:

$$CE = TED \times \frac{1}{1-LL} \times \sum_j\sum_k\sum_l\sum_m \left[FM_j \times UT_{jk} \times CT_{jkl} \times CHP_{jklm} \times HR_{jklm} \times EF_j\right] \tag{3}$$

Where subscripts j, k, l and m represent fuel type, unit type, cooling technology and CHP or non-CHP units, respectively; $CE$is the total CO_2 emissions by power generation; $TED$is the total electricity demand; LL is the grid line loss rate of electricity supply; $FM_j$is the percentage of net electricity generation using fuel j; UT_{jk} is the percentage of unit type k in net electricity generation by fuel j; $CT_{jkl}$is the percentage of cooling technology l in net electricity generation by fuel j and unit type k;CHP_{jklm} is the percentage of CHP (or non-CHP) unit type m in net electricity generation by fuel j, unit type k and cooling technology l; $HR_{jklm}$is the group-averaged heat rate by fuel j, unit type k and cooling technology l and CHP unit type m; $EF_j$is the emission factor of fuel j, which is fixed over time. All these variables were calculated based on the bottom-up emission inventory developed in this study. Changes in total CO_2 emissions between two years (t_1 and t_0) can be decomposed into changes in seven factors according to Eq. (4):

$$\begin{aligned}
CE^{t_1} - CE^{t_0} &= \Delta CE \\
&= \Delta CE_{TED} + \Delta CE_{LL} + \Delta CE_{FM} + \Delta CE_{UT} + \Delta CE_{CT} + \Delta CE_{CHP} + \Delta CE_{HR} \\
&= \sum_j\sum_k\sum_l\sum_m L\left(CE^{t_1}_{jklm}, CE^{t_0}_{jklm}\right) \times \ln\left(\frac{TED^{t_1}}{TED^{t_0}}\right) \\
&+ \sum_j\sum_k\sum_l\sum_m L\left(CE^{t_1}_{jklm}, CE^{t_0}_{jklm}\right) \times \ln\left(\frac{LL^{t_1}}{LL^{t_0}}\right) \\
&+ \sum_j\sum_k\sum_l\sum_m L\left(CE^{t_1}_{jklm}, CE^{t_0}_{jklm}\right) \times \ln\left(\frac{FM^{t_1}_j}{FM^{t_0}_j}\right) \\
&+ \sum_j\sum_k\sum_l\sum_m L\left(CE^{t_1}_{jklm}, CE^{t_0}_{jklm}\right) \times \ln\left(\frac{UT^{t_1}_{jk}}{UT^{t0}_{jk}}\right) \\
&+ \sum_j\sum_k\sum_l\sum_m L\left(CE^{t_1}_{jklm}, CE^{t_0}_{jklm}\right) \times \ln\left(\frac{CT^{t_1}_{jkl}}{CT^{t_0}_{jkl}}\right) \\
&+ \sum_j\sum_k\sum_l\sum_m L\left(CE^{t_1}_{jklm}, CE^{t_0}_{jklm}\right) \times \ln\left(\frac{CHP^{t_1}_{jklm}}{CHP^{t_0}_{jklm}}\right) \\
&+ \sum_j\sum_k\sum_l\sum_m L\left(CE^{t_1}_{jklm}, CE^{t_0}_{jklm}\right) \times \ln\left(\frac{HR^{t_1}_{jklm}}{HR^{t_0}_{jklm}}\right)
\end{aligned} \tag{4}$$

Where ΔCE_{TED}, ΔCE_{LL}, ΔCE_{FM}, ΔCE_{UT}, ΔCE_{CT}, ΔCE_{CHP} and ΔCE_{HR} represent changes in the total CO_2 emissions attributed to the seven factors. The calculator $L\left(CE^{t_1}_{jklm}, CE^{t_0}_{jklm}\right)$is given as:

$$L\left(CE^{t_1}_{jklm}, CE^{t_0}_{jklm}\right) = \begin{Bmatrix} \dfrac{CE^{t_1}_{jklm} - CE^{t_0}_{jklm}}{\ln CE^{t_1}_{jklm} - \ln CE^{t_0}_{jklm}}, CE^{t_1}_{jklm} \neq CE^{t_0}_{jklm} \\ CE^{t_1}_{jklm}, CE^{t_1}_{jklm} = CE^{t_0}_{jklm} \end{Bmatrix} \tag{5}$$

Variables equal to zero were substituted with a very small number in the calculation, for example,10^{-20}.

4. Results

4.1. Dramatic structural changes and fuel efficiency improvement

The comprehensive bottom-up dataset captures detailed plant-by-plant and unit-by-unit heat rate and CO_2 emissions in China's power sector from 1997 to 2022. It covers an average of 98.8 % of China's overall electricity generation and 98.6 % of non-nuclear thermal power generation, including coal, natural gas, oil, and other combustible fuels (Supplementary Fig. 1). This level of detail allows us to reconstruct the complete historical evolution of China's power sector at the EGU level. We observe significant structural changes and dramatic scale expansion in China's power sector over the past 26 years. The total net electricity generation increased from 1050 TWh in 1997 to 8310 TWh in 2022 (by 7.9 times), while the total real GDP (measured in Chinese yuan, CNY) increased by 15 times over the same period. One notable historical trend is the diversification of fuel mix (Fig. 1a). The share of non-nuclear thermal power decreased from 80.3 % in 1997 (842 TWh) to 64.9 % in 2022 (5392 TWh). Hydropower, as the largest renewable power source, remained at around 16–20 % (194 TWh in 1997 and 1349 TWh in 2022) during the study period. The deployment of wind power started to accelerate after 2008, followed by solar photovoltaic (PV) after 2012. These two types of non-hydro renewables amounted for 14.1 % (1175 TWh) of the total generation in 2022. In thermal power generation, coal-fired power remains dominant, accounting for more than 89 % through 2022. However, the share of other fuels, except for oil, increased to varying extents. This includes natural gas (2.75 %, 228 TWh), recovered gases (0.66 %, 54.5 TWh), municipal solid wastes (1.23 %, 102 TWh), biomass (0.65 %, 54.1 TWh) and residual heat & pressure (1.55 %, 129 TWh) (Supplementary Fig. 2).

In recent years, China's power industry policies have focused on replacing older, small-sized EGUs with advanced large-sized units. This strategy has led to significant changes in the size structure of coal-fired EGUs (Fig. 1b). Prior to 2000, EGUs smaller than 300 MW accounted for more than 60 % of coal-fired power generation. Their output peaked in 2007 and has been declining steadily since then. On the other hand, the share of 300 MW-class units expanded quickly in the first decade of the new millennium, reaching a peak of 38.5 % (812 TWh) in 2006 and remaining around 35 % thereafter. The share of both 600 MW-class and 1000 MW-class EGUs have experienced dramatic increase since the period of post-financial crisis recovery. In 2022, the share of 600 MW-class EGUs reached 36.6 % (1764 TWh), compared to 25.1 % (606 TWh) in 2007, while the share of 1000 MW-class units reached 21.9 % (1058 TWh), compared to 0.54 % (13.2 TWh) in 2007.

After the global financial crisis, China has boosted investments in energy infrastructure, favoring advanced technology deployment. As a result, these has been a rapid shift in the structure of the coal power fleet based on EGUs' size. More than 93 % (278 GW) of the newly built 600 MW-class EGUs after 2007 are supercritical or ultra-supercritical units, which are more efficient and have lower emissions than smaller ones. Another notable structural change is the increasing share of air-cooling EGUs and combined heat and power plants (CHP). Before 2000, China had only eight 200 MW air-cooling EGUs, which were imported and constructed during the late 1980s and early 1990s. After 2005, this key

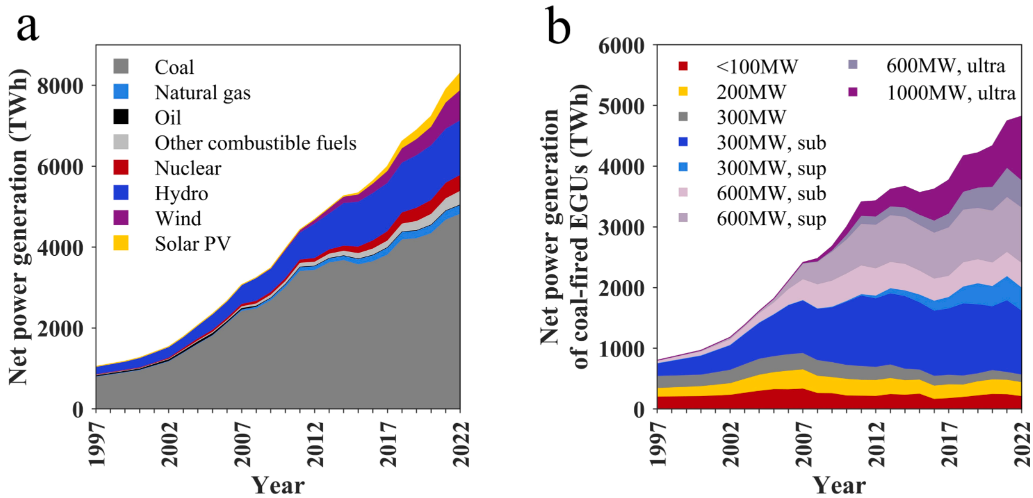

Fig. 1. Changes in overall fuel mix (a) and unit type structure of coal-fired power generation (b). Other combustible fuels in (a) include recovered gases, biomass, municipal solid wastes, residual heat & pressure. In (b), 100 MW-class covers 100–199 MW, 200 MW-class covers 200–299 MW, 300 MW-class covers 300–499 MW, 600 MW-class covers 500–999 MW, and 1000 MW-class includes all units equal to or larger than 1000 MW. **Sub** refers to the subcritical pressure level, **Sup** refers to the supercritical pressure level and **Ultra** refers to the ultra-supercritical pressure level.

water conservation technology has been deployed extensively as a countermeasure to conserve water in newly constructed coal power hubs in the arid northwestern China (NDRC, 2004; Zhang et al., 2014). The share of air-cooling EGUs in thermal power generation increased from 1.93 % in 2005 to 21.1 % in 2022 (Supplementary Fig. 3). CHP plants utilize waste heat to supply thermal energy, resulting in higher thermal efficiency compared to non-CHP plants. Many CHP plants, particularly in northern China, prioritize meeting heat demand in the heating season, and therefore have high heat-to-electricity ratio. In 2022, CHP plants provided 55.7 % (5.75 billion GJ) of urban heat supply in China while generating 25.6 % of coal-fired power (Supplementary Fig. 4).

EGU- and plant-level heat rate and CO_2 emission allow us to analyze the trends in energy efficiency and CO_2 intensity at the micro level. In contrast to the prevailing phenomenon in developed countries with aged generation fleet that energy efficiency of coal-fired power generation is relatively fixed, China has witnessed continuously declining trends in heat rate (measured in gce/kWh) and associated CO_2 emission intensity (measured in g CO_2/kWh) for almost all types of coal- and natural gas-fired EGUs. Median values of heat rate for different unit types decreased by 0.5 % to 45.1 % during the study period (Supplementary Table 5). For example, the weighted average heat rate of 300 MW-class subcritical wet-cooling non-CHP EGUs decreased from 357.4 gce/kWh in 1997 to 320.6 gce/kWh in 2022, by 10.3 %. The associated average CO_2 emission intensity decreased from 993.6 g CO_2/kWh to 891.3 g CO_2/kWh over the same period. Its air-cooling counterpart saw a decrease from 363.2 gce/kWh in 2005 to 328.8 gce/kWh in 2022, a reduction of 9.5 %. Natural gas-fired EGUs also exhibited significantly improved energy efficiency, with the average heat rate decreasing from 411.7 gce/kWh (combustion turbine) in 1997 to 220.8 gce/kWh (combined cycle) in 2021, representing a substantial decline of 46 % (Supplementary Fig. 5).

Distribution curves of heat rate for all coal-fired EGUs in 1997 (red line), 2010 (yellow line) and 2022 (blue line) are presented in Fig. 2a. The distribution curves progressively shifted downward as time went by, indicating the combined effect of structural changes and energy efficiency improvements. In 1997, the weighted average heat rate was 411.9 gce/kWh (1145 g CO_2/kWh), which decreased to 334.6 gce/kWh (951 g CO_2/kWh) in 2010 and further to 303.0 gce/kWh (842 g CO_2/kWh) in 2022. The distribution curve for 1997 exhibits a long and wide tail on the right side, indicating there were a large number of low-efficiency units during the early period. The 90th percentile of the heat rate distribution curve for 1997 is 526 gce/kWh (1462 g CO_2/kWh), and all of these low-efficiency units are smaller than 100 MW. As low-efficiency units have been gradually phased out, the tail of the distribution curve becomes thinner and steeper in the later years. In 2010, power generation from units with a heat rate higher than 411 gce/kWh only accounted for 3.6 % of the national total, and this share dropped below 0.25 % in 2022. Fig. 2b presents violin plots of unit-level heat rate categorized by unit type. There is a clear descending order in the distribution of heat rate as the nameplate capacity and main steam pressure increase. Smaller units show more dispersed distributions than larger ones due to more miscellaneous operating conditions such as varying capacity factor, heat-to-electricity ratio and mixed combustible fuels. For a specific unit type, efficiency improvement over time is also evident.

4.2. *Bottom-up reconstructed historical emission trajectory*

Using this EGU/plant level emission inventory, we reconstruct the historical CO_2 emission in China's power sector at both national and provincial levels. The total CO_2 emissions from the power sector quadrupled from 948 million tonnes (Mt) in 1997 to 4310 Mt in 2022. Coal-fired power generation contributed 94.3 % (4064 Mt) of the total emissions in 2022, a slight decrease compared to 97.0 % (919 Mt) in 1997. The emission trend exhibited some fluctuations over time. The soaring emissions observed since the late 1990s experienced a temporary pause during the global financial crisis of 2007–2008. From 2011 to 2015, there was a period of apparent stagnation, with emissions showing little growth. However, emissions rebounded and returned to their upward trajectory after 2015 (Fig. 3a). Our bottom-up emission inventory aligns well with widely used top-down estimations based on national statistical data (Supplementary Fig. 6). The correlation coefficient between the gross CO_2 emissions calculated from China's national energy balance tables and our results is 0.95. The average absolute differences in annual emissions between bottom-up and top-down estimations is 5.01 %. The largest deviation was observed in 1997 when the bottom-up accounted emission was 11.9 % (127.8 Mt) lower than the gross emission calculated based on China's national energy balance table.

At the provincial level, the emission trajectories exhibit diverse patterns. Based on whether a peak in CO_2 emissions from power generation has been reached, provinces can be divided into three groups:

1) the first group consists of provinces where peak CO_2 emission has already occurred, followed by a clear declining trend. Nine provinces

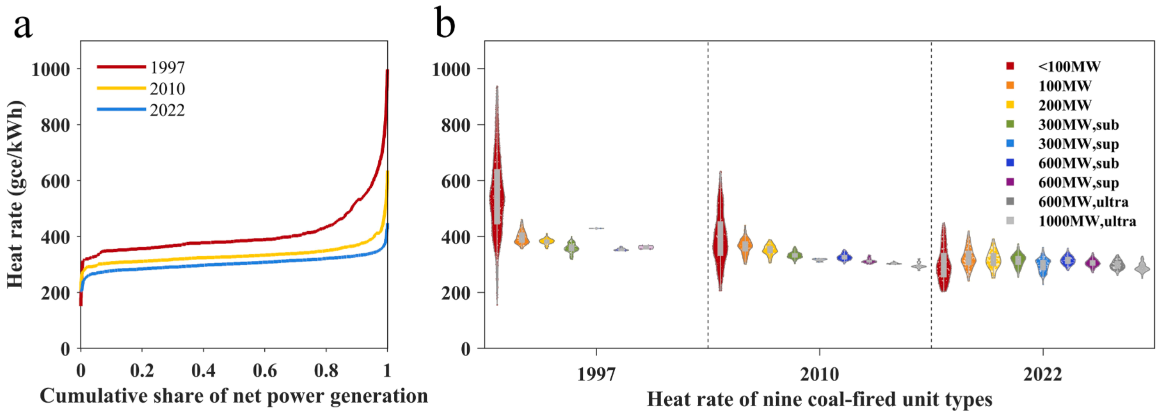

Fig. 2. Cumulative distribution curves (a) and violin plots of heat rate of coal-fired power generation (b).

belong to this group, including Beijing, Hebei, Liaoning, Jilin, Heilongjiang, Shanghai, Sichuan, and Yunnan. Newly-built coal power plants have been severely restricted in the Jing-Jin-Ji area (Beijing, Tianjin, and Hebei), as a measure to alleviate air pollution. Therefore, Beijing was the first province to retire nearly all coal power plants and reach power sector CO_2 emission peak in 2005 (24.0 Mt). A similar situation took place in Shanghai, China's largest megacity, resulting in an emission peak in 2011 (83.2 Mt). Northeast China, encompassing Liaoning, Jilin, and Heilongjiang, has gradually reduced its dependence on high-carbon energy due to the extensive development of renewable energy sources, including wind, solar PV, and nuclear power. As a result, these provinces reached emission peak in 2020, with emissions of 11.1 Mt, 49.7 Mt, and 64.6 Mt, respectively. Yunnan and Sichuan are China's top two hydropower bases located in the Southwestern region. Emission peaks in these two provinces occurred in 2009 (48.7 Mt) and 2010 (51.5 Mt), respectively, driven by massive expansion of hydropower and shrinking coal power.

2) The second group consists of provinces where emissions from the power sector are still increasing. This group includes more than half (18 in 30) of the provinces, especially those located in the eastern and southern coastal areas with rapid economic growth, as well as provinces in northwestern areas with expanding large coal mines and coal power industry hubs. Shandong is a typical example from the former category, which has the second largest volume of power sector emissions in all provinces in 2022 (370 Mt, accounting for 8.6 % of the national total). The second category is best represented by Inner Mongolia and Xinjiang, which had a twelve-fold and a twenty-four-fold increase in CO_2 emissions, respectively, over the study period.
3) Provinces in the third group have plateaued or fluctuated emission trends in recent years after an early period of growth. This group includes 4 provinces, i.e., Tianjin, Henan, Hainan and Guizhou. Taking Tianjin as an example, its CO_2 emission reached a historic high level in 2011 at 5.17 Mt, declined by more than 20 % till 2017, but rebounded to 4.7 Mt again in 2020 and 2021. Fig. 3 provides a comparison of emission trajectories for some typical provinces, and Supplementary Fig. 7 presents the trends of province-wise total net power generation, net coal power generation and CO_2 emission.

4.3. Decomposition of avoided CO_2 emissions

Changes in technological structure and energy efficiency improvements at the production-side offset a significant part of the potential increase in emissions driven by soaring final electricity consumption. With EGU/plant level technological information, we decompose the overall emission changes into seven underlying factors: 1) total final electricity consumption, 2) line loss rate, 3) fuel mix, 4) unit type structure, 5) cooling technology structure, 6) share of CHP units, and 7) grouped-average heat rate of each EGU category.

The most significant factor driving emissions to increase is the growing final electricity consumption (with transmission line loss

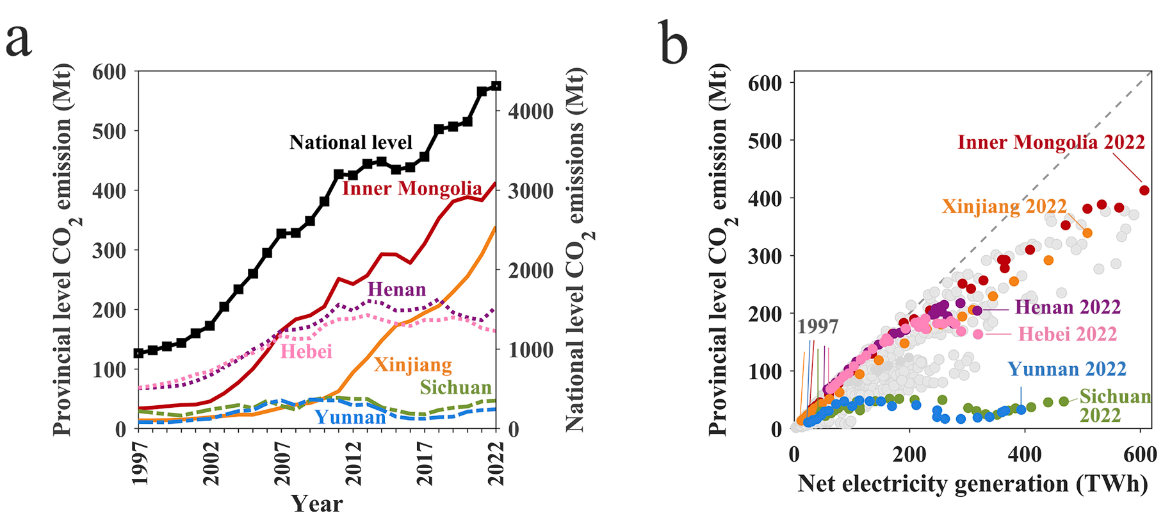

Fig. 3. Bottom-up reconstructed trajectories of CO_2 emission from power sector (a), and decoupled relationship between net electricity generation and CO_2 emissions in selected provinces (b).

deduced), which increased by more than seven-fold during the study period, from 964 TWh in 1997 to 7909 TWh in 2022. Taking 1997 as the baseline for comparison, if the national aggregate CO_2 emission intensity of per kWh electricity consumption is kept unchanged, demand increase alone could potentially lead to an additional 5073 Mt of yearly CO_2 emission for 2022. However, the weighted average CO_2 emission intensity of per unit final electricity consumption decreased from 983.3 g CO_2/kWh in 1997 to 544.9 g CO_2/kWh in 2022, by 45 %. As shown in Fig. 4a, the six technological factors collectively contributed to reducing the yearly (avoided CO_2 emissions for the year) CO_2 emission by 1710 Mt in 2022, equivalent to 39.7 % of the actual emission in 2022. The cumulative (total avoided CO_2 emissions for all years) CO_2 emission mitigation effect amounted to 15.814 billion tonnes of CO_2 throughout the study period. The year-by-year (change in avoided CO_2 emissions compared to the previous year) change in avoided CO_2 emissions is shown in Fig. 4b and the decomposition of annual CO_2 emissions including final electricity consumption is shown in Supplementary Fig. 8.

The changes in fuel mix, unit type structure, and heat rate played dominant roles in achieving the avoided emissions, which created 6055 Mt, 3661 Mt and 5527 Mt of cumulative CO_2 emission reduction. But their relative contributions over time are quite different. Fuel mix of China's power sector remained relatively stable before 2012, with coal power accounting for a percentage between 76 % and 79.2 %. Fluctuation of the percentage of coal power generation was even a contributing factor to increasing emissions before 2007. After 2012, with accelerated penetration of wind power and solar PV, changes in fuel mix achieved a tremendous decarbonization effect, reducing CO_2 emission by 889 Mt for 2022, accounting for 52 % of the yearly mitigation effect. Changes in unit type structure mainly occurred before 2012 during the period of rapid expansion of coal power capacity. Its mitigation effect amounted to 203 Mt for 2012, primarily driven by the penetration of 300 MW-class EGUs in the early 2000s and 600 MW-class EGUs in the late 2000s. The annual mitigation effect of unit type changes increased moderately to 281 Mt by 2022. Improvements in heat rate can be observed for almost all categories of EGUs/plants throughout the study period. Therefore, its contribution to decreasing CO_2 emissions grew steadily and reached 448 Mt in 2022.

Comparing to the aforementioned factors, the decrease in line loss rate, the increase in the share of air-cooling technology, and the promotion of CHP units had relatively smaller impacts. The national average line loss rate of power transmission and distribution decreased from 8.20 % in 1997 to 4.82 % in 2022, contributing 4.7 % (740 Mt) of the total cumulative avoided emission, or 104 Mt of CO_2 mitigation for 2022. In contrast, the substitution of air-cooling technology for wet-cooling technology in water scarce areas had a negative impact on carbon mitigation due to the energy penalty of this water conservation technology (Zhang et al., 2014). The yearly emission penalty is estimated to be 31 Mt for 2022. Deploying air-cooling EGUs, especially after 2005, has led to cumulative additional CO_2 emission of 340 Mt. The effect of promoting CHP units was the smallest among all factors, due to the relatively small percentage changes in power generation by CHP units (25.6 % in 2021 compared to 19.5 % in 1997). Cumulative emission mitigation adds up to 172 Mt and the yearly emission mitigation for 2022 is 21 Mt.

A comparison of the decomposition results from this study with previous researches reveals both common general trends and specific micro-level differences. Most previous studies identify macroeconomic factors related to electricity demand, such as GDP and population growth, as primary drivers to increase emissions, while improvements in energy intensity and carbon intensity are recognized as mitigating factors (Yan et al., 2019a; Zheng et al., 2020). Some studies also consider the share of thermal power in the energy mix, concluding that a reduction in thermal power share contributes to CO_2 emission mitigation (He et al., 2022; Zhang et al., 2013). Our findings align with these trends, showing that increased electricity demand led to a more than seven-fold rise in emissions during the study period, resulting in 5.86 Bt CO_2 emissions from 1997 to 2022. However, reductions in CO_2 intensity—driven by structural changes and improvements in energy efficiency—avoided 15.8 Bt CO_2 emissions over the same period. Additionally, our study provides a more detailed analysis by examining changes in the fuel mix, unit types, cooling technologies, and heat rate—areas not previously explored in the literature.

4.4. Regional disparities in driving factors

We also reveal significant spatial heterogeneities in driving factors for avoided emissions in different provinces. In general, energy resource endowment and historical capacity expansion trajectories determine provincial mitigation pathways. The structure of cumulative avoided emissions by province is presented in Fig. 5a. Jiangsu has the largest amount of aggregate avoided emission of 1701 Mt, followed by Shandong (1249 Mt) and Henan (1002 Mt). For different driving factors, a decrease in the operational heat rate contributes to CO_2 mitigation in all provinces and has the largest effect in Shandong (673 Mt), Jiangsu (604 Mt) and Shanxi (403 Mt). These three provinces are among the top producers of coal-fired power generation in China, creating large rooms for energy efficiency improvement. Although there has been a general trend of low-carbon electricity penetration, the effect of fuel mix change is inconsistent among provinces. Fuel mix change has reduced emissions

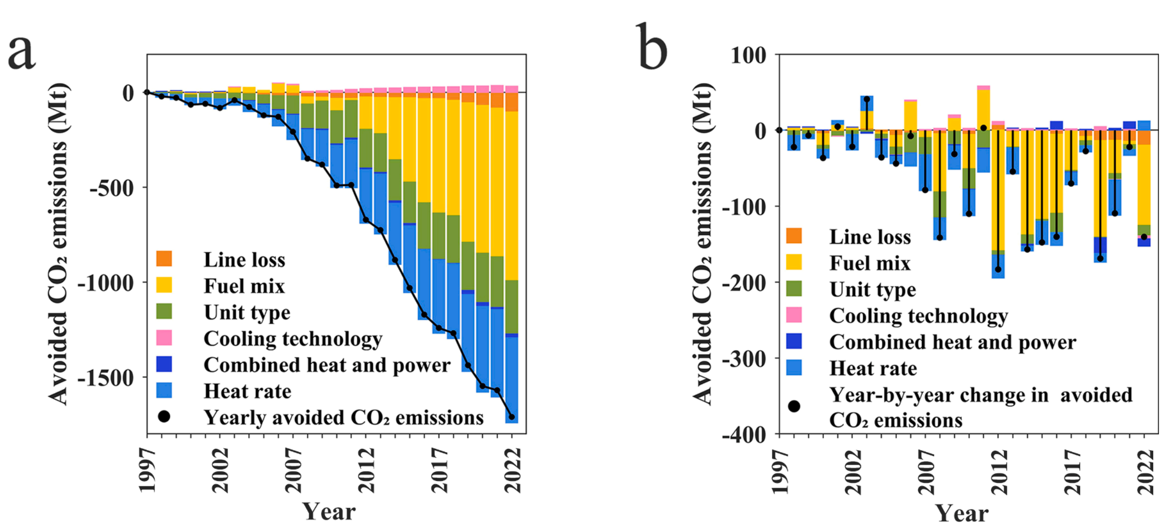

Fig. 4. Decomposition of annual avoided CO_2 emission attributed to structural changes and efficiency gain at the national level (a) and its year-by-year changes (b).

in 25 provinces. This effect is the largest in Sichuan (737 Mt), where the share of hydropower increased from 50 % in 1997 to 84 % in 2022. Avoided emission owing to fuel mix change is also significant in Jiangsu (665 Mt, due to the increased share of natural gas, nuclear power and non-hydro renewables), Inner Mongolia (496 Mt, due to the increased share of wind and solar PV) and Yunnan (494 Mt, due to increased share of hydropower). On the other hand, the percentage of coal power generation increased in five southern provinces, i.e., Hunan, Fujian, Guangxi, Jiangxi and Guangdong, resulting in negative impacts on CO_2 emission by fuel mix change. As more and more large-sized EGUs have been built to replace small ones to meet growing demand, change in unit type structure also contributed to avoided emission in all provinces, but its effect is smaller than heat rate decrease and fuel mix change. EGU structure change is the most prominent in Henan, where 600 MW-class or larger EGUs accounted for 67.5 % of its coal power generation in 2022, but none of these units was in operation before 2004. Jiangsu has thirty 1000 MW-class EGUs by 2022, which is the largest fleet among all provinces and accounts for about 16 % of the national total. Unit type change in these two provinces created 364 Mt and 271 Mt of cumulative emission mitigation in Henan and Jiangsu, respectively. Adoption of air-cooling EGUs only takes place in northwestern provinces. Installed capacity of air-cooling EGUs reached 78 % (77.0 GW) and 67.5 % (75.4 GW) of thermal power capacity in Shanxi and Inner Mongolia, respectively, leading to 63.2 Mt and 16.9 Mt of additional CO_2 emission throughout the study period due to the tradeoff effect between water conservation and carbon mitigation. Change in the share of CHP has the most diverse effect and is also negligible in most provinces. For example, it contributed to 38.8 Mt of additional CO_2 emission in Fujian and 33.6 Mt of emission reduction in Hebei.

The spatial distribution of the provincial leading driving force has notable features of geographic clustering (Fig. 5b). Decreasing heat rate plays a dominant role in 13 provinces (blue) located in four regions: 1) eastern and southern coastal provinces including Tianjin, Shandong, Zhejiang, Guangdong and Hainan; 2) Heilongjiang and Jilin in northeastern China; 3) Shanxi, Shaanxi and Xinjiang, which are three major inland coal-producing provinces; and 4) Provinces in central China such as Hunan, Hubei and Anhui. These provinces have a common feature that they have all maintained large, or even growing (e.g., Guangdong), shares of coal power generation throughout the study period, which creates enormous rooms of fuel efficiency improvement. They have

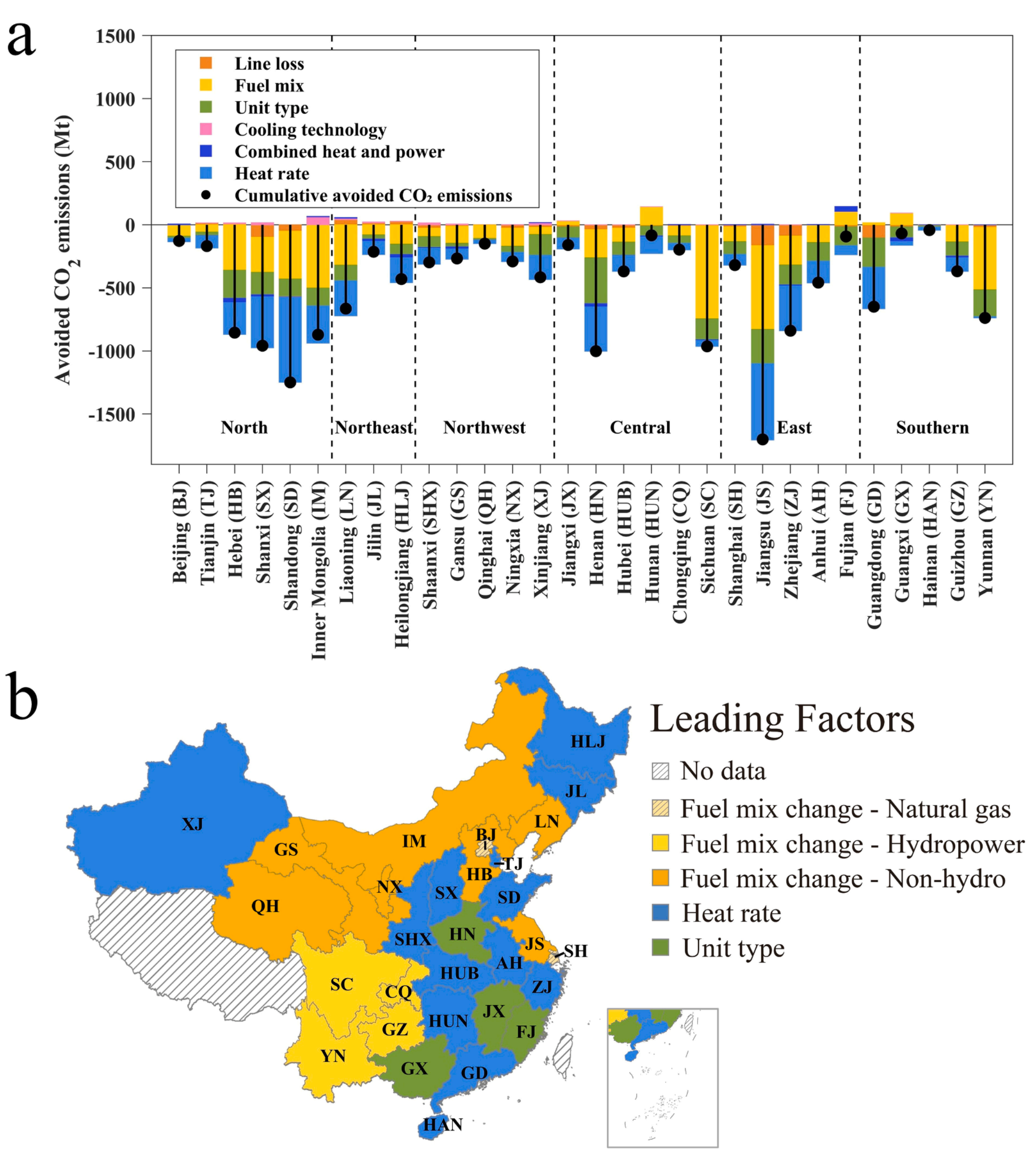

Fig. 5. Decomposition of cumulative avoided CO_2 emissions by province (a) and the spatial distribution of leading factors (b). Light yellow and dark yellow refer to fuel mix changes driven by increasing share of hydropower and non-hydro renewables, respectively. Shaded light yellow in Beijing and Shanghai means that the leading factor is increasing share of natural gas-fired power generation.

location advantages in coal availability, either with convenient sea transportation in coastal provinces or with rich local coal reserves in northeastern and northern inland regions. Power generation structure changes in these regions are not dramatic enough to outweigh the effect of continuously decreasing operational heat rate.

In contrast, western China is rich in various renewable energy resources. Therefore, mitigation pathways in western provinces depend to a larger extent on the expansion of low-carbon electricity generation. Four southwestern provinces, i.e., Chongqing, Guizhou, Sichuan, and Yunnan, located in the middle and upper reaches of the Yangtze River basin (light yellow) mainly rely on hydropower expansion to achieve avoided emissions. Sichuan and Yunnan are the top two provinces of hydropower generation, accounting for 53 % of the national total hydroelectricity output in 2022. Four northwestern provinces, i.e., Inner Mongolia, Ningxia, Gansu and Qinghai (dark yellow), are hotspot areas of large-scale wind power and solar PV deployment. Although this region also has a number of newly developed hubs of coal mines and coal power plants, especially in Inner Mongolia and Ningxia, the share of non-hydro renewable electricity quickly increased after 2012, reaching 20.5 % in Inner Mongolia, 23.4 % in Ningxia, 27.3 % in Gansu, and 41.2 % in Qinghai by 2022. Hebei and Liaoning also show non-negligible effect of fuel mix changes with rapid development of wind power and solar PV, as well as growth in nuclear power in Liaoning. Fuel mix change is also the dominant factor for CO_2 mitigation in Beijing, but with a unique feature of substituting natural gas-fired power generation for coal power for the purpose of air pollution control (Huo et al., 2023). This resulted in the most significant decline in CO_2 intensity from 886 g CO_2/kWh in 1997 to 403 g CO_2/kWh in 2022 (by 54 %), driven by a dramatic reduction of the share of coal power from 89.2 % in thermal power generation in 2005 (the highest level) to merely 2.1 % in 2022, while the share of natural gas-fired power generation increased to 91.4 % in 2022.

Unit type change is the dominant factor in four provinces including Henan, Jiangxi, Fujian and Guangxi. Henan and Jiangxi are typical provinces implementing the "Replace Small with Large" strategy which involves replacing small, inefficient, and pollution-intensive power generation units with larger, more efficient, and cleaner ones. Since 2007, these provinces have carried out extensive shutdowns of small units while expanding the installation of large-sized, high-efficiency ones. The total capacity of EGUs larger than or equal to 600 MW increased from 24.5 % (9180 MW) in 2007 to 67.3 % (44,910 MW) in 2022 in Henan, and from 29.5 % (2600 MW) to 78.2 % (20,540 MW) in Jiangxi. The commissioning of a number of large-sized EGUs can also dramatically change the unit type structure in Fujian and Guangxi in southern China, where the scale of thermal power capacity is not significant.

5. Discussion

Our analysis demonstrates that China's power sector has made continuous efforts in terms of structural change and energy efficiency improvement by applying advanced technologies and continuously improving and retrofitting coal-fired EGUs over the past two and half decades. These efforts resulted in avoided CO_2 emission of 15.8 Bt, equivalent to 23 % of the total national cumulative CO_2 emission from 1997 to 2022 (67.39 Bt). The national average CO_2 emission factor for per kWh electricity consumption in China has significantly decreased from 983.3 g CO_2/kWh in 1997 to 544.9 g CO_2/kWh in 2022 (decreased by 44.6 %). For comparison, the grid-average CO_2 emission intensity in the U.S. during the same period decreased from 645.5 g CO_2/kWh to 389.2 g CO_2/kWh, by 39.7 % (EIA, 2025).

Policy interventions have played crucial roles in driving technological upgrade and decarbonization process in China's power sector. A brief summary of national-level power sector policies and regulations, as well as associated technological factors, is presented in Supplementary Table 4. At the top level, targets for adjusting fuel mix have been set in a series of five-year plans for national energy development since 2011, which assigned expected penetration rates of renewable power. Supporting policies such as the concession bidding system and feed-in-tariffs have provided subsidies for wind power and solar PV in the early diffusion stage (NDRC, et al., 2011) and triggered technology learning effects to decrease their levelized cost of electricity (He et al., 2020).

For the carbon-intensive coal power industry, policies and regulations have focused on two aspects: upsizing coal-fired EGUs and pursuing continuous improvement in energy efficiency. The former strategy was initialized in 1999 in the policy named "Opinions on decommissioning small thermal power units", which required to shut down non-CHP coal power EGUs smaller than 50 MW (SETC, 1999). A subsequent policy promulgated in 2007 expanded the scope of decommissioning to cover 100 MW-class and 200 MW-class EGUs, and conditioned the approval of new power plant projects on the retirement of small-sized EGUs with equivalent coal consumption (NDRC, 2007). 300 MW-class non-CHP EGUs that have reached designed lifetime are required to be decommissioned in a policy issued in 2019 (NDRC, 2019).

Reducing operating heat rate plays another pivotal role in carbon mitigation. More and more stringent targets of national average heat rate of net coal power generation have been set from the 10th five-year (2001–2005) to the 14th five-year plan (2021–2025) for energy development, i.e., 380 gce/kWh by 2005, 355 gce/kWh by 2010, 323 gce/kWh by 2015, 310 gce/kWh by 2020, and 300 gce/kWh by 2025. Our analysis shows that all the targets in the 10th to 13th five-year plans have been successfully achieved, and the target in the 14th five-year plan is very likely to be reached by 2025. Two sets of energy efficiency benchmarks are assigned for different unit types: the design energy efficiency standards for newly built EGUs and the retrofit targets for existing ones. Stricter standards are stipulated for new and large-sized EGUs. For instance, in the "Action Plan for the Upgrading and Renovation of Coal Power Energy Conservation and Emission Reduction" issued in 2014, heat rate standards for newly built 600 MW-class EGUs with wet-cooling and air-cooling technology were specified as 285 gce/kWh and 302 gce/kWh, respectively, which are lower than the target for retrofitting and upgrading existing EGUs as 310 gce/kWh (NDRC, 2014). These two types of targets induce two different kinds of technology learning mechanisms for energy efficiency improvement for coal-fired EGUs, i.e., learning-by-manufacturing and learning-by-operating (Zhang et al. 2022). The former refers to performance improvement of new EGUs compared to old ones at the initial time of commissioning due to better equipment quality and system design as cumulative installed capacity grows. The latter refers to continuous heat rate reduction for individual EGUs after commissioning due to accumulation of operating and retrofitting experiences as cumulative operating hour grows.

In addition, limited coal quota is as a result of the coal consumption cap policy first introduced in three metropolitan regions (Jing-Jin-Ji, Yangtze River Delta and Pearly River Delta) in the 12th Five-year (2011–2015) Plan for Energy Conservation and Emission Reduction (CAEP, 2022 ; Han et al., 2022). A national-wide coal consumption cap of 4.1 billion tce was implemented in the subsequent 13th Five-year Plan for Energy Development. Tightened coal quota is an external pressure for energy efficiency retrofits.

It is also noticeable that policies aiming at tackling other environmental challenges the power sector is faced with could have tradeoff effect for carbon mitigation. Adopting air-cooling technology in northern and northwestern China to resolve water scarcity problem is a prominent example (Zhang et al., 2014). Air-cooling EGU has become a compulsory technology requirement in the newly developed coal power hubs in the arid northwestern provinces since 2004. We estimate that the energy penalty of air-cooling technology has resulted in a cumulative 340 Mt of additional CO_2 emission during the study period. Although this amount is quite small compared to the aggregate avoided emission, change in cooling technology structure is the only factor contributing to increasing CO_2 emission besides demand growth. Technology innovations that can narrow the efficiency gap need to be promoted, as the share of air-cooling EGUs is expected to further grow in the future. In addition, fuel switch from coal-fired to natural gas-fired thermal power generation, as a key measure to improve air quality in metropolitan areas, has brought co-benefits of air pollutants and carbon mitigation (He and Peng, 2024).

Relative contribution to carbon mitigation by alternative factors would change over time in the future. As penetration rate of renewable power technologies continue to increase, the role of fuel mix change to peak and reduce CO_2 emission in China's power sector will become more and more important (Jia et al., 2021a; Zhang and Chen, 2022). According to China's 14th five-year development plan for energy sector, the share of non-fossil electricity generation is expected to reach 39 % in 2025, compared to 33.8 % in 2020. Accelerating the deployment of wind power and solar PV has been stipulated as a top priority in developing non-fossil energy in China (Jia et al., 2021b). On the other hand, the pace of heat rate decrease of coal power generation has slowed down in recent years, as potential rooms for further improvement in energy efficiency for advanced EGUs is shrinking. Therefore, in the future, traditional energy efficiency retrofits should be transited to low-carbon retrofits for coal-fired EGUs. New measures and technologies focusing on reducing carbon intensity, rather than heat rate, need to be taken, including co-firing biomass (Wang et al., 2025), co-firing green ammonia (Sun et al., 2023), and installing carbon capture, utilization and storage (CCUS) facilities. The NDRC introduced a latest policy on these issues in June 2024, named Implementation Plan for the Retrofit and Upgrading of Coal-Fired Power Generation Units (2024–2027). According to this plan, selected pilot projects of low-carbon retrofit will start in 2025. It is expected that a 50 % reduction in carbon emission intensity should be achieved by 2027, compared to 2023 level. Government will facilitate diverse finance channels to support suitable retrofit projects and give priority in power dispatch for these power plants. Implementing these new retrofit measures on a broader scale will create vast potentials of deep carbon mitigation for traditional coal-fired power generation in the future.

6. Conclusions

This study compiles a comprehensive bottom-up dataset of heat rate and CO_2 emission intensity of individual EGUs and power plants in China. Leveraging the rich technological details in this dataset, we decompose changes in power sector CO_2 emission into more elaborated driving factors linked to specific technological policies. The high-resolution unit-level data provide new insights into how structural changes and efficiency improvements in generating units contribute to emission mitigation. This enhanced granularity enables a more precise evaluation of policy impacts, supporting the development of targeted and effective strategies for reducing emissions in the thermal power sector.

We show that fuel mix change driven by accelerated penetration of renewable power and utilization of non-coal fuels for thermal power generation has made the largest contribution to CO_2 mitigation during the past two and half decades. Continuous improvement in energy efficiency for all types of coal- and natural gas-fired EGUs regulated by periodically updated fuel consumption standards is the second largest driver. Decommissioning small coal-fired EGUs and deploying large-sized ones also made quite significant contributions. For the carbon-intensive coal-fired power generation, potential room for CO_2 mitigation by traditional energy efficiency retrofits is shrinking. In order to achieve deep mitigation in the future, it is essential to focus on low-carbon retrofits.

CRediT authorship contribution statement

Chao Zhang: Writing – review & editing, Resources, Methodology, Data curation, Writing – original draft, Project administration, Formal analysis, Supervision, Funding acquisition, Conceptualization. **Yujie Dong:** Writing – review & editing, Visualization, Formal analysis, Methodology, Data curation, Writing – original draft. **Lijin Zhong:** Conceptualization, Writing – review & editing, Data curation. **Haoqi Qian:** Data curation, Investigation, Conceptualization, Writing – review & editing. **Shuangtong Wang:** Investigation, Data curation. **Gang He:** Methodology, Writing – review & editing, Conceptualization.

Declaration of competing interest

The authors declare the following financial interests/personal relationships which may be considered as potential competing interests:

Chao Zhang and Haoqi Qian receive funding from the National Natural Science Foundation of China. Chao Zhang also receives funding from Shanghai Municipal Education Commission. Other authors declare that they have no known competing financial interests or personal relationships that could have appeared to influence the work reported in this paper.

Acknowledgments

This research is supported by the National Natural Science Foundation of China (Grant number 72174145, 72322013), Shanghai Municipal Education Commission (Shuguang Project, 21SG22), and Fundamental Research Funds for the Central Universities.

Supplementary materials

Supplementary material associated with this article can be found, in the online version, at doi:10.1016/j.ceja.2025.100812.

Data availability

The authors do not have permission to share data.

References

Ang, B.W., Goh, T., 2016. Carbon intensity of electricity in ASEAN: drivers, performance and outlook. Energy Policy 98, 170–179. https://doi.org/10.1016/j.enpol.2016.08.027.
Ang, B.W., Liu, F.L., 2001. A new energy decomposition method: perfect in decomposition and consistent in aggregation. Energy 26, 537–548. doi:10.1016/s0360-5442(01)00022-6.
Ang, B.W., Liu, F.L., Chew, E.P., 2003. Perfect decomposition techniques in energy and environmental analysis. Energy Policy 31, 1561–1566. https://doi.org/10.1016/S0301-4215(02)00206-9.
Ang, B.W., Su, B., 2016. Carbon emission intensity in electricity production: a global analysis. Energy Policy 94, 56–63. https://doi.org/10.1016/j.enpol.2016.03.038.
CAEP (Chinese Academy ofEnvironmental Planning), NRDC (Natural Resources Defense Council), 2022. Pathway for capping coal consumption in major coal consuming sectors to achieve China's carbon peaking and neutrality.
CEC, n.d.. Materials of the National Energy Efficiency benchmarking competition for coal-fired thermoelectric power generation units (2008–2020). 2008.
CEC, 2001. A list of electric generation units in operation in 2000.
CEC, n.d.. Annual compilation of statistics for power industry (1997-2021).. 1997.
CEC (China Electricity Council), 2023. China Electricity Industry Annual Development Report 2023.
Chen, G., Hou, F., Chang, K., Zhai, Y., Du, Y., 2018. Driving factors of electric carbon productivity change based on regional and sectoral dimensions in China. J. Clean. Prod. 205, 477–487. https://doi.org/10.1016/j.jclepro.2018.09.082.
Ehrlich, P.R., Holdren, J.P., 1971. Impact of population growth. Science 171, 1212–1217. https://doi.org/10.1126/science.171.3977.1212.
EIA, 2019. More U.S. coal-fired power plants are decommissioning as retirements continue.
EIA, 2015. Analysis of heat rate improvement potential at coal fired power plants. In: .
EIA (Energy Information Administration). State electricity profiles. https://www.eia.gov/electricity/state/unitedstates/state_tables.php (accessed 26 March 2025).
GEM (Global Energy Monitor), 2022. Global Coal Plant Tracker.
GEM (Global Energy Monitor), CREA, E3G, Sierra Club, SFOC, Kiko Network, CAN Europe, LIFE, Bangladesh Group; GEM (Global Energy Monitor), CREA, E3G, Sierra Club, SFOC, Kiko Network, CAN Europe, LIFE, Bangladesh Group; s, 2022. Boom and Bust 2022: Tracking the Global Coal Plant Pipeline.

Goh, T., Ang, B.W., 2020. CO_2 emissions from electricity generation in ASEAN: an empirical spatial-temporal index decomposition analysis. IOP Conf. Ser. Earth Environ. Sci. 463, 012039. https://doi.org/10.1088/1755-1315/463/1/012039.

Goh, T., Ang, B.W., Su, B., Wang, H., 2018a. Drivers of stagnating global carbon intensity of electricity and the way forward. Energy Policy 113, 149–156. https://doi.org/10.1016/j.enpol.2017.10.058.

Goh, Tian, Ang, B.W., Xu, X.Y., 2018b. Quantifying drivers of CO_2 emissions from electricity generation – Current practices and future extensions. Appl. Energy 231, 1191–1204. https://doi.org/10.1016/j.apenergy.2018.09.174.

Han, R., Li, J., Guo, Z., 2022. Optimal quota in China's energy capping policy in 2030 with renewable targets and sectoral heterogeneity. Energy 239, 121971. https://doi.org/10.1016/j.energy.2021.121971.

Hasan, M.M., Chongbo, W., 2020. Estimating energy-related CO_2 emission growth in Bangladesh: the LMDI decomposition method approach. Energy Strategy Rev 32, 100565. https://doi.org/10.1016/j.esr.2020.100565.

He, G., Lin, J., Sifuentes, F., Liu, X., Abhyankar, N., Phadke, A., 2020. Rapid cost decrease of renewables and storage accelerates the decarbonization of China's power system. Nat. Commun. 11, 2486. https://doi.org/10.1038/s41467-020-16184-x.

He, Y., Xing, Y., Zeng, X., Ji, Y., Hou, H., Zhang, Y., Zhu, Z., 2022. Factors influencing carbon emissions from China's electricity industry: analysis using the combination of LMDI and K-means clustering. Environ. Impact Assess. Rev. 93, 106724. https://doi.org/10.1016/j.eiar.2021.106724.

Heinrichs, H.U., Markewitz, P., 2017. Long-term impacts of a coal phase-out in Germany as part of a greenhouse gas mitigation strategy. Appl. Energy 192, 234–246. https://doi.org/10.1016/j.apenergy.2017.01.065.

Huo, D., Zhang, Q., Dong, Y., Kennedy, C., Zhang, C., 2023. Charging toward decarbonized electrification: revisiting Beijing's power system. Energy Strategy Rev 45, 101039. https://doi.org/10.1016/j.esr.2022.101039.

IEA (International Energy Agency), 2023. Global Energy Review: CO_2 Emissions in 2022.

IPCC (Intergovernmental Panel on Climate Change), 2006. IPCC Guidelines for National Greenhouse Gas Inventories.

Jia, J., Lei, J., Chen, C., Song, X., Zhong, Y., 2021a. Contribution of renewable energy consumption to CO_2 emission mitigation: a comparative analysis from a global geographic perspective. Sustainability 13, 3853. https://doi.org/10.3390/su13073853.

Jia, J., Rong, Y., Chen, C., Xie, D., Yang, Y., 2021b. Contribution of renewable energy consumption to CO_2 emissions mitigation: a comparative analysis from the income levels' perspective in the belt and road initiative (BRI) region. Int. J. Clim. Change Strateg. Manag. 13, 266–285. https://doi.org/10.1108/IJCCSM-06-2020-0053.

Jia, J., Xin, L., Lu, C., Wu, B., Zhong, Y., 2023. China's CO_2 emissions: a systematical decomposition concurrently from multi-sectors and multi-stages since 1980 by an extended logarithmic mean divisia index. Energy Strategy Rev 49, 101141. https://doi.org/10.1016/j.esr.2023.101141.

Karmellos, M., Kopidou, D., Diakoulaki, D., 2016. A decomposition analysis of the driving factors of CO_2 (Carbon dioxide) emissions from the power sector in the European Union countries. Energy 94, 680–692. https://doi.org/10.1016/j.energy.2015.10.145.

Karmellos, M., Kosmadakis, V., Dimas, P., Tsakanikas, A., Fylaktos, N., Taliotis, C., Zachariadis, T., 2021. A decomposition and decoupling analysis of carbon dioxide emissions from electricity generation: evidence from the EU-27 and the UK. Energy 231, 120861. https://doi.org/10.1016/j.energy.2021.120861.

Kaya, Y., 1995. The role of CO_2 removal and disposal. Energy Convers. Manag. 36, 375–380. https://doi.org/10.1016/0196-8904(95)00025-9.

Li, M., Patiño-Echeverri, D., Zhang, J., 2019. Policies to promote energy efficiency and air emissions reductions in China's electric power generation sector during the 11th and 12th five-year plan periods: achievements, remaining challenges, and opportunities. Energy Policy 125, 429–444. https://doi.org/10.1016/j.enpol.2018.10.008.

Liao, C., Wang, S., Zhang, Y., Song, D., Zhang, C., 2019. Driving forces and clustering analysis of provincial-level CO_2 emissions from the power sector in China from 2005 to 2015. J. Clean. Prod. 240, 118026. https://doi.org/10.1016/j.jclepro.2019.118026.

Liu, Z., Deng, Z., He, G., Wang, H., Zhang, X., Lin, J., Qi, Y., Liang, X., 2022. Challenges and opportunities for carbon neutrality in China. Nat. Rev. Earth Environ. (3), 141–155.

Liu, N., Ma, Z., Kang, J., 2017. A regional analysis of carbon intensities of electricity generation in China. Energy Econ 67, 268–277. https://doi.org/10.1016/j.eneco.2017.08.018.

MEP (Ministry of Environmental Protection of the People's Republic of China), 2014. A list of coal-fired power generating units equipped with desulfurization facilities.

Mohlin, K., Bi, A., Brooks, S., Camuzeaux, J., Stoerk, T., 2019. Turning the corner on US power sector CO_2 emissions—A 1990–2015 state level analysis. Environ. Res. Lett. 14, 084049. https://doi.org/10.1088/1748-9326/ab3080.

NDRC, 2014. Action Plan for the upgrading and renovation of coal power energy conservation and emission reduction (2014-2020).

NDRC, 2011. Guidelines for the compilation of provincial greenhouse gas inventory (Trial).

NDRC, 2007. Notice of several opinions on accelerating the shutdown of small thermal power units.

NDRC, 2004. Notice of the relevant requirements for the planning and construction of coal-fired power station projects.

NDRC, MOF (Ministry of Finance), NEA (National Energy Administration), 2011. Renewable Energy Development Fund Collection and Use Management Interim Measures.

NDRC (National Development and Reform Commission), 2019. Industrial Structure Adjustment Guidance Catalogue (2019 Edition).

Peng, X., Tao, X., 2018. Decomposition of carbon intensity in electricity production: technological innovation and structural adjustment in China's power sector. J. Clean. Prod. 172, 805–818. https://doi.org/10.1016/j.jclepro.2017.10.236.

Qin, X., Tong, D., Liu, F., Wu, R., Zheng, B., Zheng, Y., Liu, J., Xu, R., Chen, C., Yan, L., Zhang, Q., 2022. Global and regional drivers of power plant CO_2 emissions over the last three decades revealed from unit-based database. Earths Future 10, e2022EF002657. https://doi.org/10.1029/2022EF002657.

Raza, M.Y., Lin, B., 2022. Analysis of Pakistan's electricity generation and CO_2 emissions: based on decomposition and decoupling approach. J. Clean. Prod. 359. https://doi.org/10.1016/j.jclepro.2022.132074.

Rodrigues, J.F.D., Wang, J., Behrens, P., Boer, P.de, 2020. Drivers of CO_2 emissions from electricity generation in the European Union 2000–2015. Renew. Sustain. Energy Rev. 133, 110104. https://doi.org/10.1016/j.rser.2020.110104.

SETC, 1999. Opinions on decommissioning small thermal power units.

SETC (State Economic and Trade Commission of the People's Republic of China), 2001. 10th Five-year plan of Power industry.

Steenhof, P.A., Weber, C.J., 2011. An assessment of factors impacting Canada's electricity sector's GHG emissions. Energy Policy 39, 4089–4096. https://doi.org/10.1016/j.enpol.2011.03.056.

Sun, Y., Li, Z., Wang, Q., Zhang, J., Kong, H., 2023. Low carbon pathway and life cycle assessment of ammonia co-firing in coal power plants under the context of carbon neutrality. Ener. Convers. Manag. 296, 117648. https://doi.org/10.1016/j.enconman.2023.117648.

von Dulong, A., 2023. Concentration of asset owners exposed to power sector stranded assets may trigger climate policy resistance. Nat. Commun. 14, 6442. https://doi.org/10.1038/s41467-023-42031-w.

Wang, H., Chen, W., Bertram, C., Malik, A., Kriegler, E., Luderer, G., Després, J., Jiang, K., Krey, V., 2020a. Early transformation of the Chinese power sector to avoid additional coal lock-in. Environ. Res. Lett. 15, 024007. https://doi.org/10.1088/1748-9326/ab5d99.

Wang, J., He, S., Qiu, Y., Liu, N., Li, Y., Dong, Z., 2018. Investigating driving forces of aggregate carbon intensity of electricity generation in China. Energy Policy 113, 249–257. https://doi.org/10.1016/j.enpol.2017.11.009.

Wang, J., Li, Z., Wu, T., Wu, S., Yin, T., 2022. The decoupling analysis of CO_2 emissions from power generation in Chinese provincial power sector. Energy 255, 124488. https://doi.org/10.1016/j.energy.2022.124488.

Wang, J., Song, C., Yuan, R., 2021. CO_2 emissions from electricity generation in China during 1997–2040: the roles of energy transition and thermal power generation efficiency. Sci. Total Environ. 773, 145026. https://doi.org/10.1016/j.scitotenv.2021.145026.

Wang, Y., Yan, Q., Li, Z., Baležentis, T., Zhang, Y., Gang, L., Streimikiene, D., 2020b. Aggregate carbon intensity of China's thermal electricity generation: the inequality analysis and nested spatial decomposition. J. Clean. Prod. 247, 119139. https://doi.org/10.1016/j.jclepro.2019.119139.

Wang, Z., Sun, Y., Kong, H., Xia-Bauer, C., 2025. An in-depth review of key technologies and pathways to carbon neutrality: classification and assessment of decarbonization technologies. C. Neutra. 4 (15). https://doi.org/10.1007/s43979-025-00129-8.

Xie, P., Gao, S., Sun, F., 2019. An analysis of the decoupling relationship between CO_2 emission in power industry and GDP in China based on LMDI method. J. Clean. Prod. 211, 598–606. https://doi.org/10.1016/j.jclepro.2018.11.212.

Yan, Q, Wang, Y., Baležentis, T., Streimikiene, D., 2019a. Analysis of China's regional thermal electricity generation and CO_2 emissions: decomposition based on the generalized Divisia index. Sci. Total Environ. 682, 737–755. https://doi.org/10.1016/j.scitotenv.2019.05.143.

Yan, Q., Wang, Y., Li, Z., Baležentis, T., Streimikiene, D., 2019b. Coordinated development of thermal power generation in Beijing-Tianjin-Hebei region: evidence from decomposition and scenario analysis for carbon dioxide emission. J. Clean. Prod. 232, 1402–1417. https://doi.org/10.1016/j.jclepro.2019.05.256.

Yan, Q., Zhang, Q., Zou, X., 2016. Decomposition analysis of carbon dioxide emissions in China's regional thermal electricity generation, 2000–2020. Energy 112, 788–794. https://doi.org/10.1016/j.energy.2016.06.136.

Yang, L., Lin, B., 2016. Carbon dioxide-emission in China′s power industry: evidence and policy implications. Renew. Sustain. Energy Rev. 60, 258–267. https://doi.org/10.1016/j.rser.2016.01.058.

Zhang, C., Anadon, L.D., Mo, H., Zhao, Z., Liu, Z., 2014. Water−carbon trade-off in China's coal power industry. Environ. Sci. Technol. 48, 11082–11089. https://doi.org/10.1021/es5026454.

Zhang, C., Xie, L., Qiu, Y., Wang, S., 2022a. Learning-by-manufacturing and Learning-by-operating mechanisms drive energy conservation and emission reduction in China's coal power industry. Resour. Conserv. Recycl. 186, 106532. https://doi.org/10.1016/j.resconrec.2022.106532 (Lucy).

Zhang, C., Zhong, L., Fu, X., Zhao, Z., 2016. Managing scarce water resources in China's coal power industry. Environ. Manage. 57, 1188–1203. https://doi.org/10.1007/s00267-016-0678-2.

Zhang, C., Zhong, L., Wang, J., 2018. Decoupling between water use and thermoelectric power generation growth in China. Nat. Energy 3, 792–799. https://doi.org/10.1038/s41560-018-0236-7.

Zhang, M., Liu, X., Wang, W., Zhou, M., 2013. Decomposition analysis of CO_2 emissions from electricity generation in China. Energy Policy 52, 159–165. https://doi.org/10.1016/j.enpol.2012.10.013.

Zhang, M., Lv, T., Zhao, Y., Pan, J., 2020. Effectiveness of clean development policies on coal-fired power generation: an empirical study in China. Environ. Sci. Pollut. Res. 27, 14654–14667. https://doi.org/10.1007/s11356-020-08011-z.

Zhang, N., Zhao, Y., Wang, N., 2022b. Is China's energy policy effective for power plants? Evidence from the 12th Five-Year Plan energy saving targets. Energy Econ 112, 106143. https://doi.org/10.1016/j.eneco.2022.106143.

Zhang, S., Chen, W., 2022. Assessing the energy transition in China towards carbon neutrality with a probabilistic framework. Nat. Commun. 13, 87. https://doi.org/10.1038/s41467-021-27671-0.

Zhao, Y., Cao, Y., Shi, X., Li, H., Shi, Q., Zhang, Z., 2020. How China's electricity generation sector can achieve its carbon intensity reduction targets? Sci. Total Environ. 706, 135689. https://doi.org/10.1016/j.scitotenv.2019.135689.

Zheng, X., Lu, Y., Yuan, J., Baninla, Y., Zhang, S., Stenseth, N.C., Hessen, D.O., Tian, H., Obersteiner, M., Chen, D., 2020. Drivers of change in China's energy-related CO_2 emissions. Proc. Natl. Acad. Sci. 117, 29–36.

Zhou, G., Chung, W., Zhang, Y., 2014. Carbon dioxide emissions and energy efficiency analysis of China's regional thermal electricity generation. J. Clean. Prod. 83, 173–184. https://doi.org/10.1016/j.jclepro.2014.06.047.